Available online at www.sciencedirect.com
SCIENCE DIRECT®
Chemical Physics Letters 406 (2005) 294–299
CHEMICAL PHYSICS LETTERS
www.elsevier.com/locate/cplett

Electronic structure calculations of radical reactions for poly(methyl methacrylate) degradation

Patrick F. Conforti, Barbara J. Garrison *

Department of Chemistry, 104 Chemistry Building, Penn State University, University Park, PA 16802, United States

Received 25 January 2005; in final form 10 February 2005
Available online 23 March 2005

Abstract

The hybrid CBS-QB3 electronic structure approach is used to calculate the reaction energetics for decomposition reactions of radicals formed from UV radiation of the polymer poly(methyl methacrylate) (PMMA). Relative to the photon created radical species, the decarboxylation reaction to form CO_2 is exothermic whereas the reaction to form CO is endothermic. For degradation of the polymer in low-Earth orbit (LEO) conditions, the synergy of the reaction with $O(^3P)$ atoms is considered. The addition of O atoms to all of the radicals is exothermic, leading in many cases to the formation of a stable molecule and another radical species.

1. Introduction

Irradiation of polymeric materials by ultraviolet (UV) laser light initiates chemical reactions that change the fundamental character of the material. For industrial applications such as boring cylindrical holes in a highly integrated, multilayer printed circuit board [1,2], drilling holes for ink jet nozzles [3], stripping polymer coatings of optical fibers [4], and, most notably, laser in situ keratomileusis, or LASIK [5], the removal of material is a desirable consequence of the radiation. In contrast, materials exposed to UV light in low-Earth orbit (LEO) conditions experience degradation. Under LEO conditions, ground state oxygen atoms have high relative collision energies of approximately 5 eV with material surfaces that cause an additive effect to produce further degradation [6]. The essential chemistry of the interaction of UV light with polymeric and biological materials is that the photon energy can be sufficient to break chemical bonds [7]. Subsequently, the material decomposes into smaller molecules and gaseous products which can readily vaporize, collect under the surface, and force the removal of larger pieces of the substrate. Although the photochemistry of the specific materials is often known and the gaseous products can be measured, the microscopic details of the chemistry and physics from the photon created radicals to the final measured products are not well understood.

Understanding the overall process of material removal due to UV radiation requires a complex model that incorporates the heterogeneity of the system as well as the energetics of the material. Our group has been simulating UV effects on materials by developing a model that follows the spirit of a kinetic Monte Carlo (KMC) method where the thermodynamics (activation and reaction energies) are utilized for a reaction in the system, and incorporates the dynamics of the particles through the classical equations of motion [8]. Although reaction energetics have been calculated for some photoproducts [9], more information is needed about the reaction barriers and energies of radical decomposition to implement our model.

In order to study of the effect of UV radiation, the polymer poly(methyl methacrylate), or PMMA, has been selected due to its use in commercial applications, such as in pulsed laser deposition [10] and as a satellite material [11]. When a UV photon interacts with

* Corresponding author. Fax: +814 863 8403.
E-mail addresses: bjg@psu.edu, bjg@chem.psu.edu (B.J. Garrison).

0009-2614/$ - see front matter © 2005 Elsevier B.V. All rights reserved.
doi:10.1016/j.cplett.2005.02.124

PMMA, several chemical reactions are possible as shown in Fig. 1a [12]. For the Norrish Type II process, a bond in the main chain is cleaved which leads to the appearance of smaller polymer chains and monomer units, MMA. The cleavage of the ester side chain (either Norrish Type I or ester elimination) gives other possible products such as carbon dioxide, carbon monoxide, methyl formate, and methane, as well as leading to cross linking of the polymers. At short wavelengths (157 and 193 nm), the Norrish Type II reaction dominates, and the main product yields are MMA monomers and lower molecular weight PMMA chains [13,14]. With a wavelength of 248 nm, the Norrish Type I reaction dominates and products such as C_2, CO, CO_2, methanol, methyl formate, and the MMA monomer are detected in the ablation plume [15,16]. Using 260 and 266 nm radiation, the ablation plume yields MMA, CO_2, CO, methyl formate, as well as MMA minus the methyl formate or methyl groups [17]. With 308 nm radiation, MMA dimers are observed [18]. Under LEO conditions, oxygen atoms can also interact with PMMA radical material to form C=O bonds as well as epoxide rings [19,20].

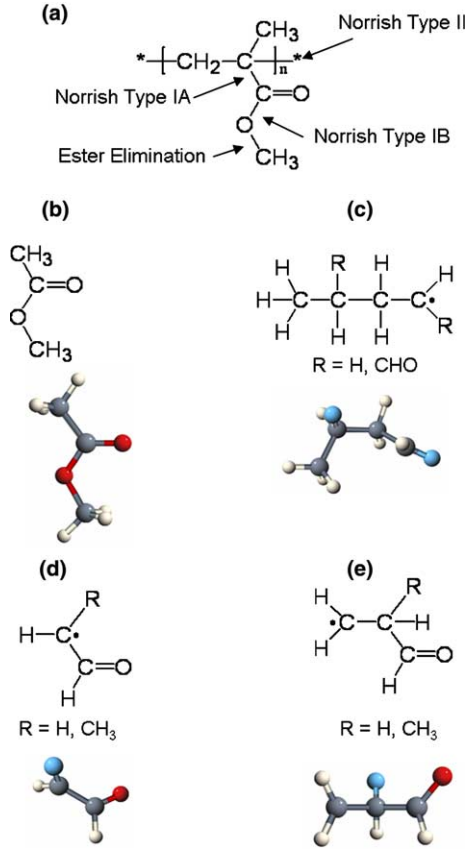

Fig. 1. Structure of compounds used in the simulations. (a) Photochemistry of PMMA, (b) methyl acetate, (c) ethylene dimer radical (R = H) or 2-propenal dimer radical (R = CHO), (d) ethanal (R = H) radical or propanal ($R = CH_3$) radical, (e) propanal (R = H) radical or isobutanal ($R = CH_3$) radical. In the models, C atoms are grey, O atoms red, H atoms white and R groups turquoise.

In the present work using high-level electronic structure calculations, we investigate the reaction pathways for the decomposition of the bond cleavage products of PMMA as shown in Fig. 1a as well as the interaction of oxygen atoms with the radical species. The objective is to obtain reasonable estimates of the reaction barriers and energies for use in studies of ablation and degradation of PMMA. Previous calculations by Stoliarov et al. [9] have yielded total reaction energetics of the decomposition of several model compounds based on PMMA, including several alkanes and carbonyls, into smaller molecular weight compounds and CO_2. To complete the description of the interaction of the various wavelengths of light and oxygen with PMMA, we need to calculate the reaction barriers to form various products and calculate the reaction energies to produce oxygenated molecules and gaseous CO. We acknowledge that the polymer sample is a much more complex and heterogeneous environment than the gas phase reactions under investigation. In addition, we ignore the details of the initial photon absorption event, assuming that the bond cleavage event will occur, and, therefore, the starting points for consideration are the resulting radical species. An exquisite investigation of the Norrish Type I bond cleavage of gas phase acetone demonstrates the intricacies involved after the photon absorption [21]. Below, we discuss the computational model, the results of the electronic structure calculations, a brief speculation of the ramifications of these results on the material degradation processes, and the utilization of the results for molecular dynamics studies.

2. Computational details

The objective of these investigations is to obtain realistic values of reaction barriers of radical reactions of relevance to UV irradiated and oxygen bombarded PMMA. The processes of interest include elimination of CO and CO_2 (decarboxylation) from the radicals formed from the Norrish Type I and ester elimination reactions; unzipping of homopolymers due to the Norrish Type II bond cleavage; and reaction of O atoms with the Norrish products. Previous electronic structure investigations of PMMA used the hybrid CBS-QB3 approach to calculate reaction enthalpies [9]. The mean absolute deviation of energies calculated with the CBS-QB3 method are within 4.2 kJ mol^{-1} of the experimental energies [22]. This level of agreement is deemed sufficient given that the ultimate system of interest is a solid polymer with a very heterogeneous environment. Thus, the CBS-QB3 hybrid method as implemented in the GAUSSIAN 03 quantum chemistry program [23] is used to obtain the reaction barriers and energies. As discussed below, density functional theory (DFT) calculations

are used to estimate the effect of delocalization through the side chain on the unzipping reaction. Complete active space self-consistent field (CASSCF) calculations have been utilized to study the reactive surface of the decarboxylation reactions in which the initial radical contains a delocalized π system. In each case, the transition states are verified by the presence of imaginary vibrational frequencies and intrinsic reaction coordinate (IRC) analyses.

Model compounds that retain the key chemistry of PMMA are utilized in the electronic structure calculations. The Norrish Type I and ester elimination reactions are modeled with methyl acetate (Fig. 1b) which has the essential bond functionality of a MMA monomer. The hybrid CBS-QB3 method is used for this calculation. In the case of the Norrish Type IA bond cleavage, the resulting radical has a delocalized π system over the O–C–O functional group. Since the resulting product of CO_2 has orthogonal π bonds, a multi-configuration reference state is needed. We use the CASSCF calculation that considers the nine electrons and nine orbitals, CAS(9,9), involved in the decarboxylation reaction with a diffuse 6-311+G(d,p) basis set. The Norrish Type II and unzipping reactions are modeled with dimers of the homopolymer polyethylene (Fig. 1c). The reaction energetics are calculated with both the density functional B3LYP/6-311+G(d,p) and the CBS-QB3 method. In order to determine the possible effects of a delocalized π bond including the side chain in MMA, the unzipping of a 2-propenal dimer radical was calculated at the B3LYP/6-311+G(d,p) level of theory. Reactions between an oxygen atom and the products of the Norrish Type I cleavage are modeled with the radicals resulting from the photon interaction with methyl acetate and $O(^3P)$ at the CBS-QB3 and, in the case of the decarboxylation reactions from a delocalized π system, the CASSCF levels of theory. Similarly the interaction of atomic oxygen (^3P) with the products of the Norrish Type II cleavage are modeled with ethanal, propanal, and isobutanal radicals using the CBS-QB3 approach (Fig. 1d and e).

3. Results and discussion

3.1. Norrish type I and ester elimination reactions

The results of the various gas phase Norrish Type I and ester elimination reactions of methyl acetate (structure 1) at the CBS-QB3 and the CASSCF levels of theory to yield CO_2, CO, $^{\cdot}OCH_3$, and $^{\cdot}CH_3$ at 298 K are given in Fig. 2a. The initial bond cleavage energetics to form structures 2, 3, and 4 are similar with structure 2 being resonance stabilized by the delocalized π system. Relative to the radical species, the formation of CO_2 is exothermic with barriers of 50 and 57 kJ mol^{-1} whereas the formation of CO is endothermic with barriers of 94 and 68 kJ mol^{-1}.

Our calculation of the enthalpy change of the decarboxylation reaction from structure 3 to structure 9 is the same as the previous calculation by Stoliarov et al. [9]. Since we used the CASSCF level of theory, the decarboxylation reaction from structure 2 to structure 9 differs by 10 kJ mol^{-1} from that reported by Stoliarov et al. [9] (−72 kJ mol^{-1}), who utilized the CBS-QB3 method for the calculation of reaction enthalpy.

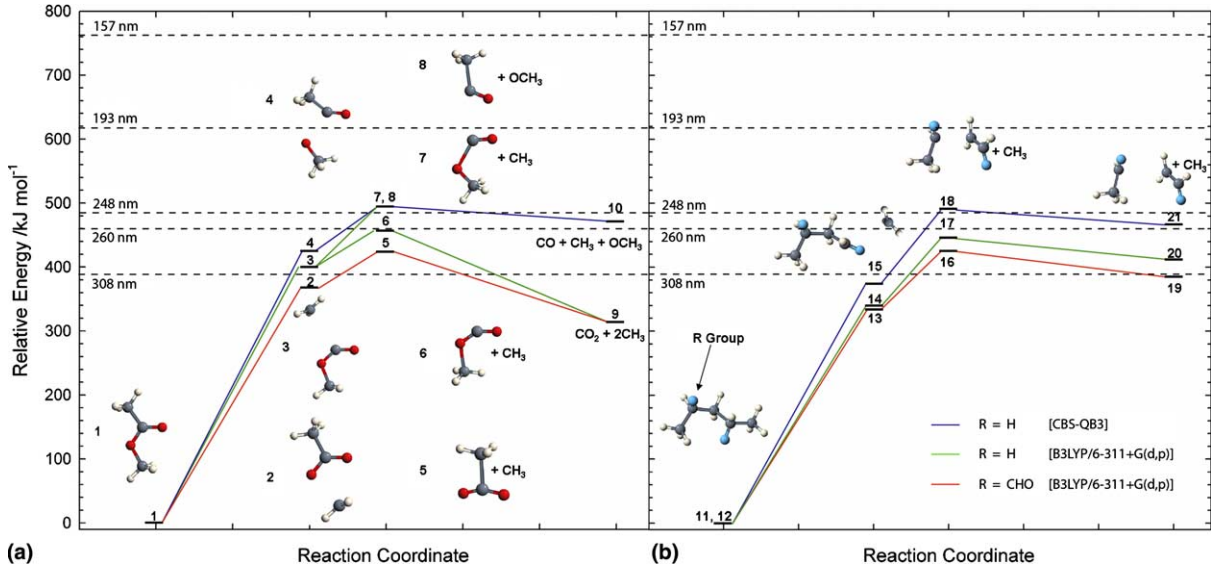

Fig. 2. Reaction energetics. (a) Methyl acetate, CH_3COOCH_3, decomposition at the CBS-QB3 and CASSCF levels of theory (298 K). (b) Cleavage of a C–C bond in a polyethylene dimer (blue and green reaction paths) and 2-propenal dimer (orange reaction path). All energies are relative to the energy of the methyl acetate molecule. For discussion purposes, the energies of several common UV laser wavelengths are denoted.

3.2. Norrish type II and unzipping reactions

The results of the unzipping reactions of a polyethylene dimer radical (structures 14, 15) to produce an ethyl radical and an ethylene molecule at the CBS-QB3 and DFT levels of theory are given in Fig. 2b. In addition, energetics calculated with DFT for the unzipping of a 2-propenal dimer radical (structure 13) to form a 2-propenal radical and 2-propenal are shown. Each reaction is calculated relative to starting structures 11 and 12, where a C–C bond must be cleaved in order to form the radical dimers. All three results are qualitatively similar. The overall reaction is endothermic and all reactions are activated relative to the cleaved structures 13, 14 and 15. Comparing the effect of delocalization of the π system into the side chain, the reaction barriers differ by 15 kJ mol^{-1}. The lower energy for the formation of 2-propenal and 2-propenal radical is due to the delocalized π system that occurs across the C═C–C═O bonds, allowing it to be more stable than ethylene. The unzipping reaction of the polyethylene dimer radical calculated with the CBS-QB3 method ($15 \rightarrow 21$) is 6 kJ mol^{-1} more endothermic than the same reaction calculated with DFT ($14 \rightarrow 20$). The major difference in the two levels of theory is the bond dissociation reaction (structure 12 to structure 14 or 15).

3.3. Oxygen and norrish type reactions

Oxygen interactions with each of the products of the Norrish Type I and ester elimination radicals (structures 22–26) of the model compound methyl acetate calculated with the CBS-QB3 and CASSCF methods are presented in Fig. 3. In each case, the O atom binds to the radical in an exothermic reaction. Addition of oxygen to structure 24 to yield structure 29 corresponds to addition to a radical on a C atom to form methoxy radical. Addition of oxygen to structures 22 and 23 leads the

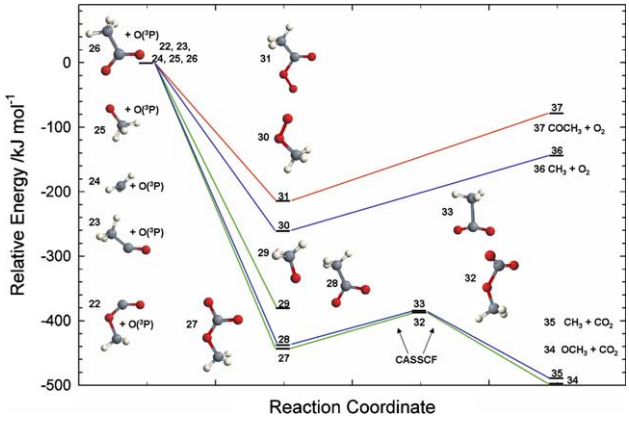

Fig. 3. Energetics of oxygen reactions with Norrish Type I radicals at the CBS-QB3 and CASSCF levels of theory (298 K).

metastable structures 27 and 28 with subsequent loss of CO_2 releasing a total of 450–500 kJ mol^{-1}. Production of O_2 occurs from the addition of the O atom to structures 25 and 26 with the release of 60–150 kJ mol^{-1}. The pathways to produce O_2 vs. CO_2, however, proceed through intermediate structures which are lower in energy than the resulting compounds.

The energetics of the interaction of oxygen with model Norrish Type II products are shown in Fig. 4. In the first case, the bond cleavage reaction occurs at the C atom adjacent to the side chain and the model compounds are an ethanal radical (39) and a propanal radical (structure 38), as shown in Fig. 4a. In the second case, the bond cleavage is not at the adjacent C atom, and the model compounds are a propanal radical (47) and an isobutanal radical (46) as shown in Fig. 4b. In both cases, the reactions are exothermic by 200–300 kJ mol^{-1}. There are, however, intermediate structures (40, 41, 48 and 49) that are lower in energy than the final products.

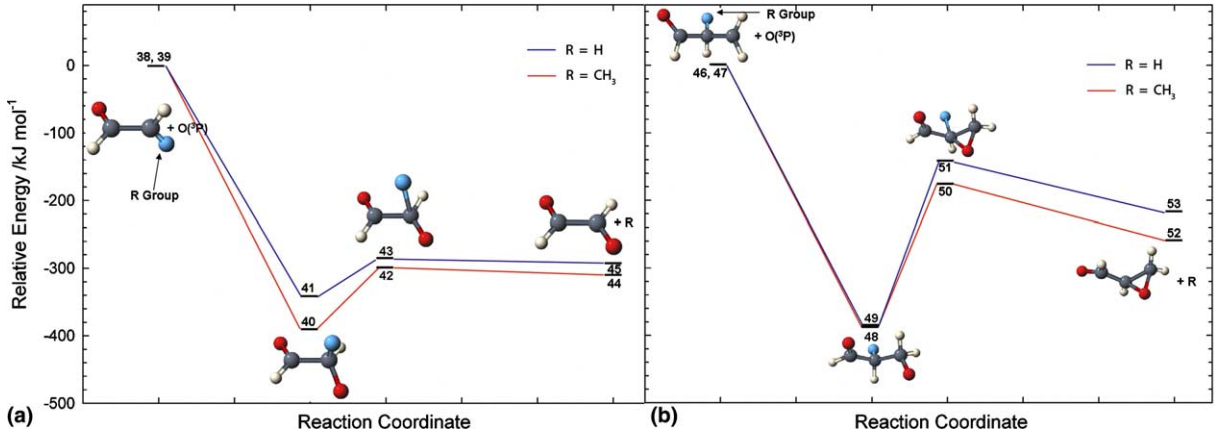

Fig. 4. Energetics of oxygen reactions with Norrish Type II radicals. (a) ethanal radical (blue path) and propanal radical (orange path) at the CBS-QB3 level of theory (298 K), (b) propanal radical (blue path) or isobutanal radical (orange path) at the CBS-QB3 level of theory (298 K).

3.4. UV irradiation

In order to assess the importance of the heights of the reaction barriers, the photon energies for several commonly used lasers are shown in Fig. 2. The mechanism of the photon energy deposition is unknown, and thus the discussion below is based completely on energetics. The discussion also ignores the absorptivity of the material at each wavelength. At the shorter wavelengths of 157 nm (762 kJ mol^{-1}) and 193 nm (620 kJ mol^{-1}), sufficient energy is available to surmount the reaction barriers to yield the eventual products of CO_2, CO, $^{\cdot}CH_3$, and $^{\cdot}OCH_3$. The energy barrier, approximately 62 kJ mol^{-1} for the unzipping of compounds 13, 14, and 15, could also be surmounted at these shorter wavelengths. At the wavelengths of 248 nm (482 kJ mol^{-1}) and 260 nm (460 kJ mol^{-1}), the amount of energy supplied by the UV light can overcome the reaction barriers to form CO_2, but it is approximately 12–34 kJ mol^{-1} less than that necessary to form CO. The compulsory energy, though, can be supplied from other exothermic reactions that are occurring during the irradiation event, or supplied from the energy transfer during molecular collisions. Since the decomposition reactions do not have sufficient energy from the photon, the radical species should exist for some time and have the potential to abstract an H atom to form the observed products of methanol and methyl formate. For the wavelength of 308 nm (388 kJ mol^{-1}), there is insufficient energy to overcome the reaction barriers to form CO, CO_2, $^{\cdot}OCH_3$, or $^{\cdot}CH_3$ or to unzip the chain to form the experimentally determined MMA monomer products.

3.5. O bombardment

The direct reactions of 5 eV $O(^3P)$ atoms with small hydrocarbon chains has been investigated by Schatz and co-workers [24–26] using an ab initio dynamics methodology. They find that the energetic O atom can abstract H atoms to form OH, directly cleave bonds to form methoxy ($^{\cdot}OCH_3$) plus another radical as well as form a ketone with two free H atoms. These reactions form, in general, radical species. Similarly, the UV photons create radical species and the issue is what happens next. The calculations presented in Fig. 3 represent scenarios of the O atom reaction with the radical remaining on the polymer chain and/or the fragment side chain. Reactions 24–29, 23–28 and 26–31 represent O addition reactions on the polymer side of the bond cleavage, which subsequently are followed by the loss of CO_2 (reactions 28–35) and loss of O_2 (reactions 31–37). In two out of the three scenarios, the polymer is etched when a small gas molecule is formed. Reactions 24–29, 22–27 and 25–30 represent O addition reactions on the fragment side of the bond cleavage, which subsequently are followed by the loss of CO_2 (reactions 27–34) and loss of O_2 (reactions 30–36). In two out of the three scenarios, a stable gas molecule is formed. The penetration depth of the 5 eV O atom probably does not extend much beyond the first one or two layers, thus two-thirds of the O atom absorption events to a radical site will lead to formation of a small molecule, such as O_2 or CO_2, that is positioned to desorb from the surface. In Fig. 4, the elimination of each R group could either represent the removal of the H atom or methyl radical from the polymer chain, or represent the removal of a full valence molecule and the radical R group could correspond to the rest of the polymer chain. The newly formed molecules have one to four C or O atoms from the original polymer, thus one incident O atom has the potential to remove several times its mass. The energy released from the reaction could then be harnessed to initiate further reactions in the polymeric material. In addition, the O atom has ~5 eV of kinetic energy, which provides more energy for chemical reaction pathways.

4. Conclusions

The ramifications of the calculated reaction energetics on the materials processes are complex and are intertwined with the specific conditions. In laser ablation, the photons irradiate the sample in a relatively short period of time, at most on the order of nanoseconds. As reactions proceed, heterogeneities in the material temperature, pressure and concentration can arise. On the other hand in LEO conditions, the time between the arrival of individual photons and O atoms is on the order of seconds. In order to assess the relative importance of these various reactions under different conditions, they will be incorporated into molecular dynamics (MD) simulations used previously to model the complex phenomenon of laser ablation of molecular solids [27–30]. The specifics of the reaction barriers and overall energetics will be implemented through the coarse grained chemical reaction model (CGCRM) [8].

Acknowledgments

This work was supported by the US Air Force Office of Scientific Research through the Multi-University Research Initiative and the National Science Foundation through the Information Technology Research program. The computer support was provided by the Academic Services and Emerging Technologies at Penn State University. We also appreciate the thoughtful discussions with Yaroslava Yingling, Mark Maroncelli, Chester Swalina and R. Srinivasan.

Appendix A. Supplementary data

Table S1, the quantitative energy changes associated with each of the reactions and Cartesian coordinates for the optimized stationary points are given. Supplementary data associated with this article can be found, in the online version, at doi:10.1016/j.cplett.2005.02.124.

References

[1] F. Bachmann, Chemtronics 4 (1989) 149.
[2] J.R. Lankard, G. Wolbold, Appl. Phys. A 54 (1992) 355.
[3] J.H. Brannon, T.A. Wassick, Proc. SPIE 2991 (1997) 146.
[4] F. Barnier, P.E. Dyer, P. Monk, H.V. Snelling, H. Rourke, J. Phys. D 33 (2000) 757.
[5] C. Gorman, TIME (1999).
[6] K. Gotoh, M. Tagawa, N. Ohmae, H. Kinoshita, Colloid Polym. Sci. 279 (2001) 214.
[7] R. Srinivasan, V. Mayne-Banton, Appl. Phys. Lett. 41 (1982) 576.
[8] Y.G. Yingling, B.J. Garrison, J. Phys. Chem. B 108 (2004) 1815.
[9] S.I. Stoliarov, P.R. Westmoreland, M.R. Nyden, G.P. Forney, Polymer 44 (2003) 883.
[10] H.-U. Krebs, M. Weisheit, J. Faupel, E. Süske, T. Scharf, C. Fuhse, M. Störmer, K. Sturm, M. Seibt, H. Kijewski, D. Nelke, E. Panchenko, M. Buback, Adv. Solid State Phys. 43 (2003) 505.
[11] L.E. Murr, S. Quinones, J.M. Rivas, J. Liu, C.S. Niou, B. Marquez, A.H. Advani, in: W.R. KanneJr, G.W.E. Johnson, J.D. Braun, M.R. LouthanJr. (Eds.), Microstructural Science, International Metallographic Society, Columbus, 1993, p. 243.
[12] W.A. Noyes Jr., in: P.G. Ashmore, F.S. Dainton, T.M. Sugden (Eds.), Photochemistry and Reaction Kinetics, Cambridge University Press, Cambridge, 1967, p. 1.
[13] T.H. Fedynyshyn, R.R. Kunz, R.F. Sinta, R.B. Goodman, S.P. Doran, J. Vac. Sci. Technol. B 18 (2000) 3332.
[14] R. Srinivasan, B. Braren, D.E. Seeger, R.W. Dreyfus, Macromolecules 19 (1986) 916.
[15] G.B. Blanchet, P. Cotts, C.R. Fincher, J. Appl. Phys. 88 (2000) 2975.
[16] D.J. Krajnovich, J. Phys. Chem. A 101 (1997) 2033.
[17] R.C. Estler, N.S. Nogar, Appl. Phys. Lett. 49 (1986) 1175.
[18] M. Tsunekawa, S. Nishio, H. Sato, J. Appl. Phys. 76 (1994) 5598.
[19] L. Lianos, D. Parrat, T.Q. Hoc, T.M. Duc, J. Vac. Sci. Technol. A 12 (1994) 2491.
[20] J. Song, C.H. Fischer, W. Schnabel, Polym. Degrad. Stab. 36 (1992) 261.
[21] E.W.G. Diau, C. Kotting, A.H. Zewail, ChemPhysChem 2 (2001) 273.
[22] G.A. Petersson, in: J. Cioslowski (Ed.), Quantum-mechanical Prediction of Thermochemical Data, Kluwer Academic Publishers, Boston, 2001.
[23] M.J. Frisch et al., Gaussian 03, Revision B.05, Gaussian, Inc., Pittsburgh, PA, 2003.
[24] D.J. Garton, T.K. Minton, D. Troya, R. Pascual, G.C. Schatz, J. Phys. Chem. A 107 (2003) 4583.
[25] D. Troya, R.Z. Pascual, G.C. Schatz, J. Phys. Chem. A 107 (2003) 10497.
[26] D. Troya, G.C. Schatz, J. Chem. Phys. 120 (2004) 7696.
[27] L.V. Zhigilei, P.B.S. Kodali, B.J. Garrison, J. Phys. Chem. B 101 (1997) 2028.
[28] L.V. Zhigilei, E. Leveugle, B.J. Garrison, Y.G. Yingling, M.I. Zeifman, Chem. Rev. 103 (2003) 321.
[29] L.V. Zhigilei, B.J. Garrison, J. Appl. Phys. 88 (2000) 1281.
[30] L.V. Zhigilei, Y.G. Yingling, T.E. Itina, T.A. Schoolcraft, B.J. Garrison, Int. J. Mass. Spectrom. 226 (2003) 85.